

This is the peer-reviewed version of the article:

Krueger, E., Popović-Maneski, L., Nohama, P., 2018. Mechanomyography-Based Wearable Monitor of Quasi-Isometric Muscle Fatigue for Motor Neural Prostheses. *Artificial Organs* 42, 208–218. <https://doi.org/10.1111/aor.12973>



This work is licensed under the [Attribution-NonCommercial-NoDerivatives 4.0 International \(CC BY-NC-ND 4.0\)](https://creativecommons.org/licenses/by-nc-nd/4.0/)

Mechanomyography-Based Wearable Monitor of Quasi-Isometric Muscle Fatigue for Motor Neural Prostheses

*†Eddy Krueger, ‡Lana Popovic-Maneski, and †§Percy Nohama

**Neural Engineering and Rehabilitation Laboratory, Universidade Estadual de Londrina, Londrina;*

†*Universidade Tecnológica Federal do Parana, Curitiba, Brazil;*

‡*Institute of Technical Sciences of the Serbian Academy of Sciences and Arts, Belgrade, Serbia; and*

§*Graduate Program in Health Technology, Pontificia Universidade Catolica do Parana, Curitiba, Brazil*

Abstract: A motor neural prosthesis based on surface functional electrical stimulation (sFES) can restore functional movement (e.g., standing, walking) in patients with a spinal cord injury (SCI). sFES generates muscle contractions in antigravity muscles and allows balance-assisted standing. This induced standing has several benefits, such as improved cardiovascular function, decreased incidence of urinary infections, reduced joint contractures, and muscle atrophy. The duration of sFES assisted standing is limited due to the quick onset of muscle fatigue. Currently, there is no method available to reliably estimate real-time muscle fatigue during sFES. Simply monitoring the M-wave changes is not suitable due to the high signal disturbances that arise during multi-channel electrical stimulation. Mechanomyography (MMG) is immune to electrical stimulation artifacts and can be used to detect subtle vibrations on the surface of the skin related to activation of the underlying muscle's motor units (MU). The aim of this study was to develop a method for detecting muscle fatigue brought on by sFES. The method was tested in three different heads of the quadriceps muscle in SCI patients during electrically elicited quasiisometric contraction. Six spinal cord-injured male volunteers, with no voluntary control of the quadriceps muscle participated in the study. Electrical bursts of voltage-controlled monophasic square pulses at frequencies of 1 kHz (50% duty cycle) at 50 Hz (15% duty cycle) were used to generate thigh muscle contractions that controlled the knee joint in the sagittal plane. The pulse amplitudes were set to position the knee joint at a 58° angle from the horizontal plane and when the knee angle dropped to 208° (e.g., the quadriceps were unable to hold the lower leg in the desired position), the test was terminated. Two data segments lasting 10 s each, at the beginning and end of each test, were analyzed. The muscle contraction was assessed by MMG sensors positioned on the *rectus femoris*, *vastus lateralis*, and *vastus medialis* muscles. Data segments were decomposed into 11 frequency bands using a Cauchy wavelet transform. In the initial time interval (non-fatigued muscle), the power peak was concentrated in the 11.31 Hz frequency band. In the final interval (muscle fatigued) this peak shifted to lower frequencies (2 and 6 Hz frequency bands). The decreased frequency was most prominent during the last 4 s of the recordings. It was shown that MMG could be used as a real-time indicator of muscle fatigue during FES-induced isometric contraction of quadriceps; hence, MMG could be used in closed-loop control as a fatigue detector. Subsequent studies for non-isometric contractions could possibly lead to prediction of muscle fatigue before contractile failure during functional use of the muscle.

Keywords: Mechanomyography, Wavelet, Functional electrical stimulation, Spinal cord injury, Muscle fatigue

Spinal cord injury (SCI) affects motor and sensory functions (1) below the lesion level (2). Depending on the severity it can be referred to as partial or complete. Common causes for a SCI are traffic and diving accidents, urban violence, and other physical disorders (3). Functional electrical stimulation (FES) can be used to generate functional movements in humans after SCI (4–6) by the controlled application of electrical pulses to neuromuscular pathways (7). Systematic FES contributes to the overall health of the SCI population through musculoskeletal, cardiac, metabolic, and psychological gains (8–11). The biggest problem in the effective use of FES for the restoration of standing and walking is the induced muscle fatigue. The rapid onset of muscle fatigue during FES occurs due to the non-physiological activation of muscle fibers (12–15). Various attempts have been carried out to reduce FES-induced fatigue, such as modulation of the stimulation parameters (13,16–18) or switching of stimulation pulses over multiple motor points of the same muscle at lower frequencies (19,20). For switching control, real-time wearable systems for monitoring the fatigue level are required.

It is most convenient to monitor muscle fatigue during isometric contraction with force/torque transducers (21) or an electrogoniometer (22). However, measurable force or movement is the result of simultaneous activation of multiple synergistic muscles and does not represent the activity level of a single muscle accurately. Electromyography (EMG) is correlated with the muscle force, thus surface recordings of the EMG is an appealing alternative to the measurement of the force, especially in the case of motion. However, when high FES amplitudes are required (e.g., for standing and walking, pulse voltage higher than 150 V or pulse current >100 mA) EMG recordings become highly contaminated with stimulation artifacts, and as such are not suitable for real-time detection of muscle fatigue. Typical applications include: (a) in SCI patients, EMG can only be used to assess the decrease of M wave intensity as an indicator of muscle fatigue (23,24) because there is no voluntary activation of the muscles; (b) during multi-channel FES with equidistant bursts (e.g., four channels set to 16 Hz each (25)) and high pulse amplitudes, EMG signals become contaminated with stimulation artifacts on approximately 15 ms; (c) the onset of a M wave appears between 0 and 10 ms after a stimulation pulse (for distances up to 40 mm between stimulating and recording electrodes) and it lasts approximately 5–10 ms (26); (d) according to Chesler and Durfee (23) and Mizrahi et al. (24), EMG blanking procedures for artifact removal lead to the loss of useful signal for a duration of approximately 5–10 ms after each stimulation pulse (or burst). From a–d, it is clear that EMG cannot be used as a fatigue indicator during multi-channel distributed stimulation, which was shown to be highly beneficial for the reduction of muscle fatigue (19,25,27). Therefore, there is no currently available method for reliable real-time monitoring of paralyzed muscle fatigue during FES in the form of a wearable device. However, when using a lower extremity neural prosthesis, online monitoring of muscle fatigue and a real-time alert of fatigue development is essential for preventing falls during standing and walking due to a sudden contractile failure of the muscle (28–30). Both therapists and patients would benefit from such a

monitor, which could allow them to safely optimize training or use of FES for ambulation.

One feasible way to acquire the muscle activity when using FES is mechanomyography (MMG). MMG is a technique used to measure mechanical vibrations of muscles during a contraction. MMG is a mechanical signal and, therefore, not contaminated by electrical signals from FES (31). Several studies have already investigated the applicability of MMG for the assessment of muscle fatigue (32,33), mainly from studying the decrease in median frequency (MF) of the power spectral density (PSD) and the increase of the root mean square signal amplitude (RMS). However, nearly all of these studies were conducted in healthy volunteers and without electrical stimulation (34–36). As an exception, Decker et al.

(37) used MMG to assess muscle fatigue in SCI patients during FES cycling and showed the opposite trend of RMS amplitudes. The differences are expected because of the differences in motor unit (MU) recruitment strategies in the case of physiologically and electrically elicited contractions (38), as well as the inability of the paralyzed muscle to activate additional muscle fibers throughout fatigue development. We hypothesized that subtle vibrations on the surface of the skin were related to the activation of the underlying muscle fibers and that both frequency and amplitude will decrease with advancing fatigue due to the electrically elicited contraction of the completely paralyzed muscle.

The Cauchy wavelet transform (CaW) (39), based on continuous wavelet transform, originally developed for the analysis of electromyographic signals, may be used with the MMG technique after adjustments in the time and frequency resolution (40). As such, CaW appears to be suitable for analysis of the MMG signal during FES application to a SCI subject, making it an important analysis tool because it can track frequency variations during neuromuscular physiological changes with higher fidelity than with FFT or classic CWT using linearly scaled wavelets (41).

The goal of this study was to investigate fatigue properties of the quadriceps muscle (superficial group) in paraplegics during exhaustive quasiisometric contraction elicited by FES, using the Cauchy wavelet transform of MMG signals.

TABLE 1. *Spinal cord injury information for the participants*

Subject	Spinal cord injury			
	Etiology	Level	Months	ASIA
1	Diving	C5–6(I)	167	B
2	Car accident	T4–5(C)	24	A
3	Car accident	T3(C)	60	A
4	Car accident	T4–5(C)	194	A
5	Spinal cord cancer	T10(I)	3	B
6	Car accident	T4(C)	29	A

C: complete; I: incomplete; ASIA: American Spinal Injury Association impairment scale (A–E).

SUBJECTS AND METHODS

Subjects

The experimental study was approved by Human Research Ethics Committee of Pontificia Universidade Catolica do Parana (PUCPR) under register number 2416/08. Six volunteers with SCI (Table 1) participated in the study (age: 32.6 \pm 8.8 years [mean \pm SD], weight: 92.3 \pm 40.5 kg [mean \pm SD], and height: 1.6 \pm 0.4 m [mean \pm SD]). All patients signed the informed consent form approved by the Ethics Committee. A physical evaluation was performed to check participants' American Spinal Injury Association (ASIA) impairment scale (2), as shown in Table 1. Only patients with complete motor dysfunction below the lesion level were included (ASIA A and B). The exclusion criteria were: participants classified as ASIA C, D, or E, cancer in the lower limb (stimulated area), participants who have been submitted to X-ray examination in the last 2 weeks (aversion), those having implanted devices in the stimulated limb, or those with a cognitive impairment. One subject was excluded due to sensibility intolerance during FES application.

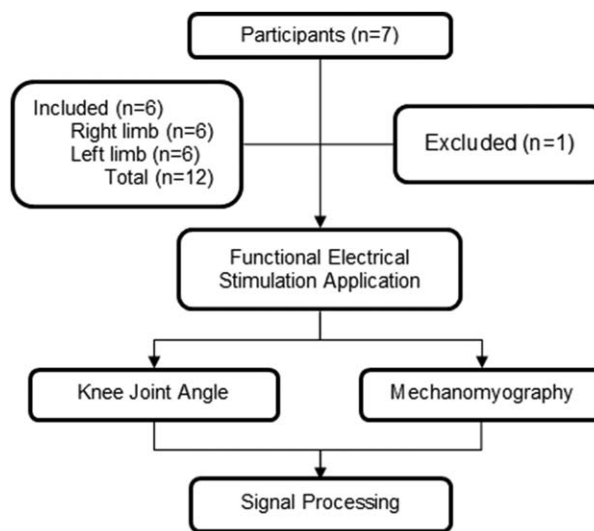


FIG. 1. Flowchart with the steps of the protocol.

During the clinical study, the subjects did not use any medication that would change their motor condition or reduce spasticity. The ASIA A volunteers did not show the zone of partial preservation and all of them were classified as level “0” in the quadriceps muscles (no voluntary contraction). Reflex assessment results were as follows: the third volunteer performed as level “0” (no reflex) while the others were graded as “1” (reduced reflex) or “2” (normal reflex) at both sides ($N = 12$, lower limbs). The subjects were not previously trained with FES. A flowchart of the experimental protocol is shown in Fig. 1.

Electrical stimulation parameters

The voltage-controlled electrical stimulator delivered monophasic square pulses with adjustable amplitude. The pulse frequency was set at 1 kHz (50% duty cycle) with a burst frequency of 50 Hz

(3 ms active burst duration and 17 ms with no activity, i.e., 15% duty cycle) as illustrated in Fig. 2. This type of stimulation, usually referred to as Russian Stimulation, showed several benefits compared with typical FES stimulation, in that higher training rate of the muscles with more comfort is achieved. Typical burst frequency usually described in the literature was 50 Hz, and carrier frequency of 1 kHz produced the highest torques and less fatigue but less comfort than 10 kHz carrier (42) (this is important only when applied to subjects with preserved sensory function). The existing literature indicates that no optimal duty cycle for carrier frequency has been established; however, there are several implications that the duty cycle less than 20% leads to optimum torque production with less electrical charge delivered to the tissue (43), and therefore, less fatigue or possibility of tissue damage.

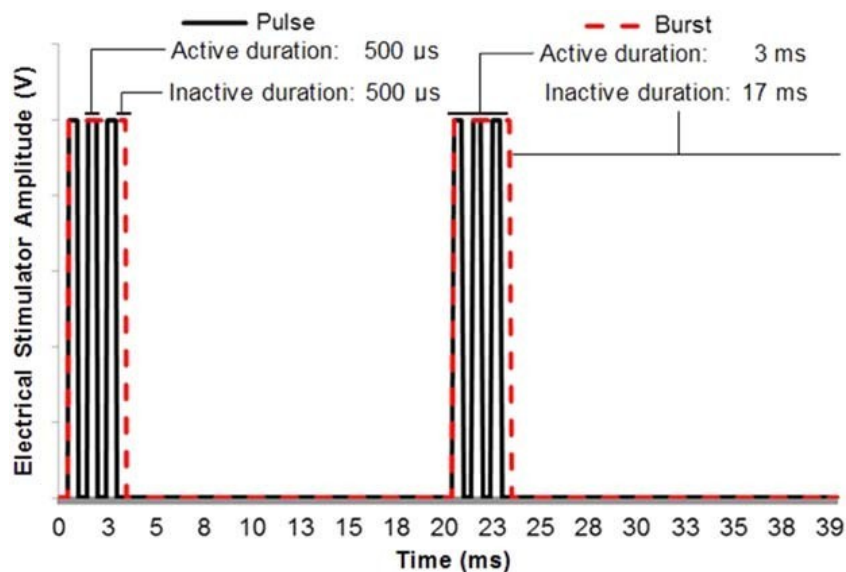


Fig. 2. Electrical stimulation parameters and waveform profile. High-frequency pulses (1 kHz) were modulated in bursts at low-frequency (50 Hz). The pulse intensity can be set between 0 and 250 V.

The protocol was performed on different limbs on different days (at least 2 days apart) with the limb (right or left) selected randomly on the first day. Self-adhesive electrodes of two different sizes were positioned on the thigh over the knee (5 3 9 cm anode) and over the femoral triangle (5 3 5 cm cathode) to stimulate the quadriceps muscles via the femoral nerve (44).

Sensors and data acquisition

The developed MMG virtual instrumentation used a Freescale MMA7260Q MEMS triaxial accelerometer (13 3 18 mm, 0.94 g) with sensitivity set to 800 mV/g. Only the X-axis was used to register the lateral (transverse) displacement of the muscle belly. The electronic circuits provided 103 amplification. A LabVIEW interface was created to acquire and visualize MMG signals. The acquisition system included a DT300 series Data Translation board operating at a 1 kHz sampling rate. A customized electrogoniometer was used to register the knee angle.

Transducer placement

After preparing the skin by means of trichotomy and cleaning, MMG sensors were positioned over the quadriceps muscle bellies – rectus femoris (RF), vastus lateralis (VL), and *vastus medialis* (VM) – using double-sided adhesive tape. The sensor placed on the RF was equidistant between the anterosuperior iliac spine and top of the patella. The sensor over the VL was equidistant between the greater trochanter and the lateral condyle of the femur, while the sensor over the VM was placed in the medial third distal thigh region. The electrogoniometer was fixed (with elastic bands) laterally to the knee joint axis (lateral epicondyle). Figure 3 shows the positions of sensors and electrodes.

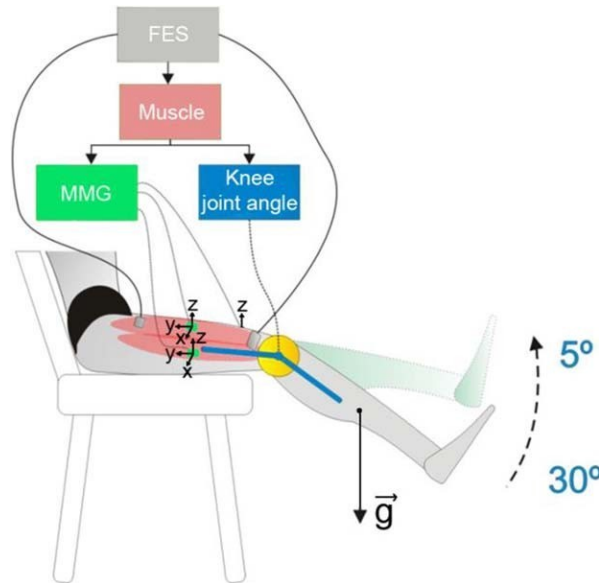


Fig. 3. Experimental setup. FES electrodes were positioned on the thigh over the knee region and the femoral triangle. MMG sensors were positioned over the *rectus femoris*, *vastus lateralis*, and *vastus medialis* muscle bellies, where only the X-axis signal was processed. The electrogoniometer was fixed laterally to the knee joint.

Experimental protocol

During the measurements, temperature and humidity were 20.4 ± 3.18°C and 61.1 ± 4.9% (mean ± SD), respectively. The volunteers were seated comfortably with the hip angle flexed at approximately 70° with their thigh resting on the bench. After attaching electrodes on the limb, sub-threshold motor electrical stimuli were applied during a 10-min session. Subsequent repetitions of rising, plateau and decay phases (10 s each) were applied to increase the neural excitability (45) and balance the skin-electrode impedance (46) before measuring the fatigue. The maximum knee extension (passive movement) was defined as the knee angle of 0°. The initial knee joint flexion was 30°. The FES intensity was increased to reach and keep the knee joint angle around 58° (Fig. 3). The 58° angular position was chosen to avoid maximum extension to keep track of the force produced by quadriceps opposed to gravity. The stimulation generated the knee joint torque to compensate gravity of the shank and foot. When the knee joint angle exceeded 20° for at least 5 s, the measurement was terminated (fatigued muscle). The moment when the knee exceeded 20° was considered as the end of the protocol.

Data processing and analysis

MMG signals were processed with a third order Butterworth pass-band filter in the range from 5 to 100 Hz. Two segments were selected from each MMG signal for further analysis. The initial segment (non-fatigued) was defined as the 4 s duration signal after the transient signal that followed the onset of FES (movement artifact due to knee extension). The final segment (fatigued) started 7 s and ended 3 s before the end of the protocol (knee joint angle greater than 208), as illustrated in Fig. 4. The initial and final segments were visualized and selected through BioProc2 version 2 and processed through MatLab version R2008a. The signals were processed in 11 frequency bands by Cauchy wavelet (CaW) transform (39) (2, 6, 11, 19, 28, 39, 51, 65, 81, 99, and 119 Hz) and the root mean square (in epochs of 1 s) was computed for each CaW frequency band for both segments. To visually emphasize signal variations, data in each frequency band were normalized by the values of the signal during the first second of the initial (non-fatigued) segment. For each recording and each muscle head, diagrams were shown for both non-normalized and normalized data.

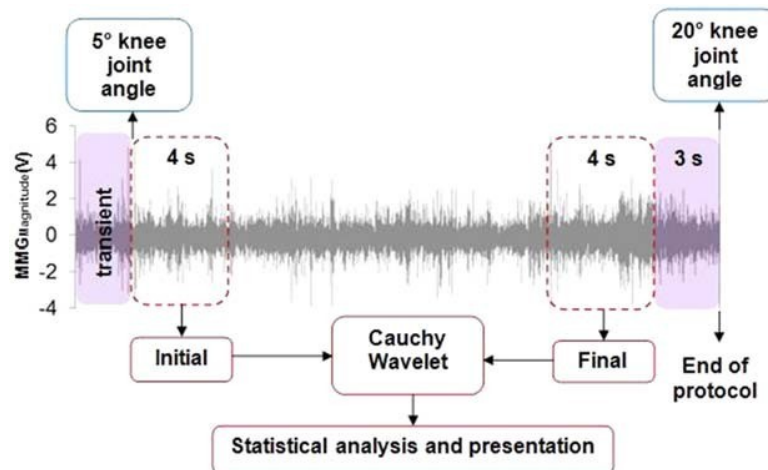


Fig. 4. Example of MMG signal segments used for Cauchy wavelet processing. The initial segment is defined as the first 4 s of recording after stabilization of the knee (movement artifact) when the muscle is in the non-fatigued state, and the final segment is defined as 4 s of recording that ends 3 s before the end of the protocol (knee angle exceeded 208).

Statistical analysis

The statistics were calculated with the software PASW Statistics version 18. Due to the small sample size, non-parametric statistics was applied. The Wilcoxon signed-rank test was used to verify the difference between the CaW frequencies power in the initial and final segment. When P value was lower than 0.05, the result was considered statistically significant. Standard deviation or interquartile ranges were used to show the variations among results. Effect size (d) was calculated (47) for all data.

RESULTS

The maximum FES pulse intensity required to keep the knee joint flexed at 58° in each FES profile was: 187.33 ± 50.36 V (mean ± SD for peak amplitude). The knee joint angle in initial and final instants was 5.98 ± 4.718 (mean ± SD) and 19.95 ± 2.318 (mean ± SD), respectively. The interval between the initial and final segment was 82.94 ± 43.22 s (mean ± SD).

Figures 5–7 illustrate the bidimensional MMG time-frequency responses calculated from non-normalized and normalized data from the RF, VL, and VM, respectively. In the color bars, dark red represents the maximal output amplitudes (for each sensor) and white the amplitudes lower than 10% of the maximal output. In the non-normalized data graphs it is clear that MMG frequency content during FES application is always below 60 Hz; therefore, the MMG signal was not affected by the 60 Hz of the electrical network.

In the initial segment (non-fatigued), the greatest power (peak) was at approximately 11 Hz. In the final segment (fatigued), the power peaks were located at pseudo-frequencies of 2 and 6 Hz, mainly during the last seconds of recordings (7th, 8th, 9th, and 10th). The box plot representations of different frequency bands in both data segments are shown in Figs. 8 and 9.

Figure 10 shows the results of the Wilcoxon signed-rank test for each CaW frequency band between the initial and final segments and the effect size for each of them. There were statistically significant differences in all muscles for the frequency bands involving 28 and 51 Hz (50 Hz modulated-frequency). There is insufficient statistical significance to prove the consistence of energy shift to lower frequencies in the fatigue instant, possibly due to large interquartile deviation values in Figs. 8 and 9.

DISCUSSION

According to the literature, for isometric contraction motor unit firing rates range from 20 to 50 Hz approximately. Within this bandwidth, slow fibers contract at lower and fast fibers at higher frequencies (48). According to Bellemare et al., volitional contraction at 50 Hz approaches the maximum physiologic capacity of motor unit contraction. When FES burst (modulated) frequency is set to 50 Hz there is an expected energy concentration at the applied frequency band (around 51 Hz). However, when the muscle is non-fatigued, our results suggest that there is a peak energy concentration at 11 Hz. Nashmi and Fehlings' study (49) with spinal cord injured rats showed that there is a decrease in axon's diameter and myelination ratio in the ventral column (motoneurons locus), resulting in slower conduction velocity and a longer refractory period. Assuming that such changes occur in humans, it is hypothesized that the greatest energy around 11 Hz observed in the three MMG sensors during FES burst frequency at 50 Hz may be related to motoneuron inability to deliver such frequency to the muscle cell, even in the case of the fastest motor unit neuron in the body (quadriceps muscle).

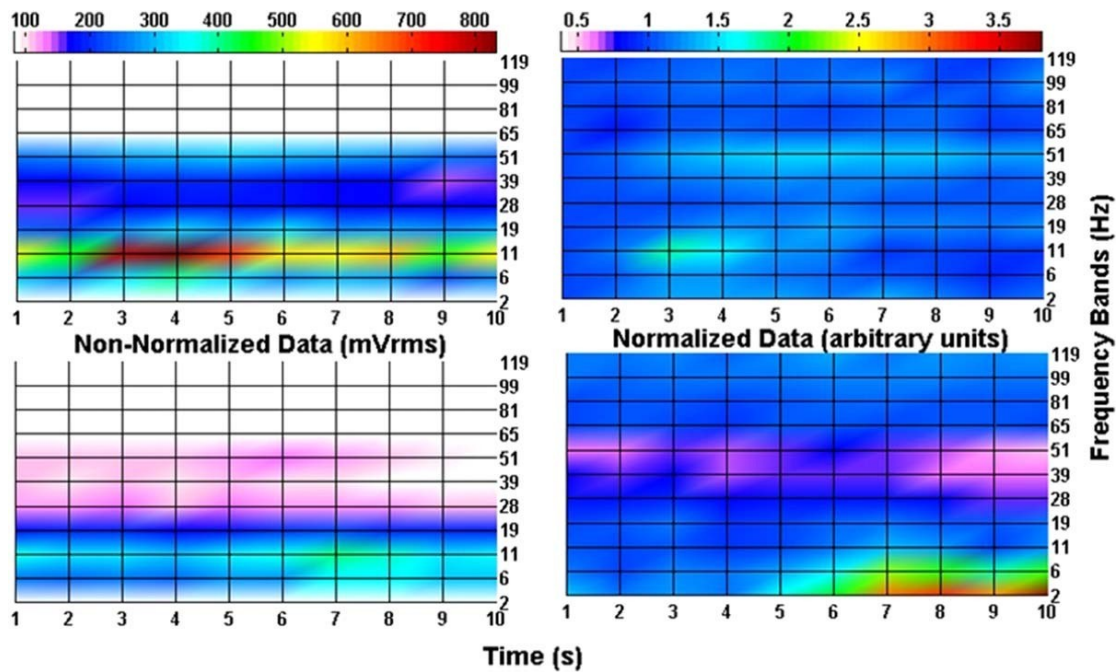


Fig. 5. The 2D MMG time-frequency responses (averaged) from the rectus femoris muscle during FES-induced isometric contraction: non-normalized (left image) and normalized (right image) data. In the top images: the initial segment followed by additional 6 s (non-fatigued); in the bottom images: the final segment with previous 6 s (fatigued). For the non-normalized data: dark red color on the color bar represents the maximum value (831 mVrms), and white color represents the values below 10% of the maximum (83.1 mVrms). In the normalized data: dark red color on the color bar represents the maximum value (3.8 arbitrary units) and white color represents the values below 10% of the maximum (0.38 arbitrary units).

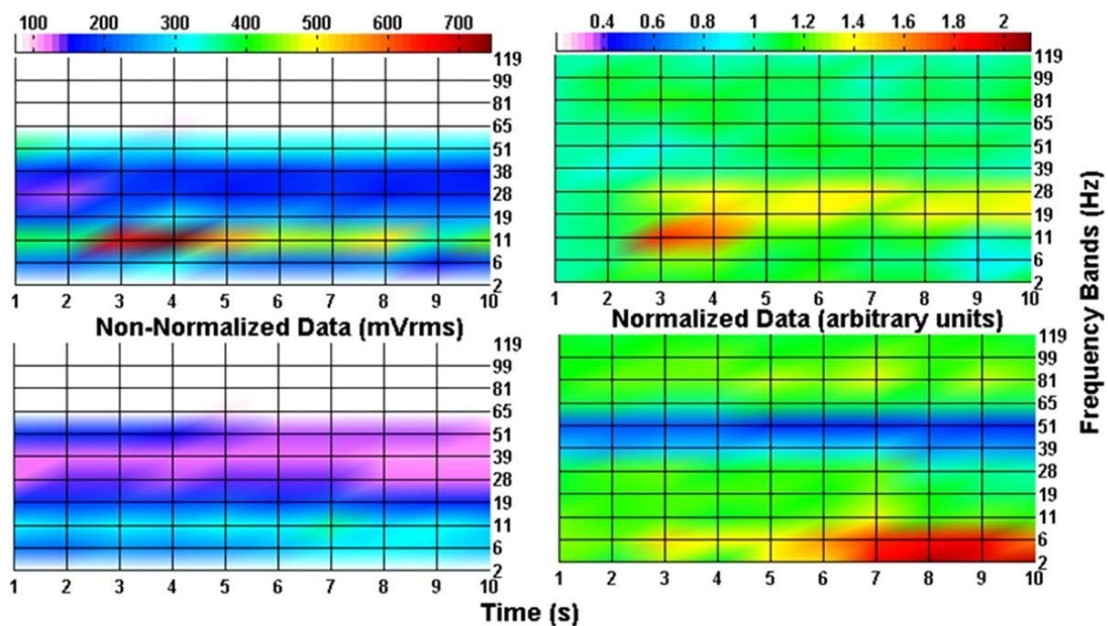


Fig. 6. The 2D MMG time-frequency responses (averaged) of the vastus lateralis muscle during FES-induced isometric contraction: non-normalized (left image) and normalized (right image) data. In the top images: the initial segment followed by additional 6 s (non-fatigued); in the bottom images: the final segment with previous 6 s (fatigued). In non-normalized data: dark red color on the color bar represents the maximum value (745 mVrms), and white color represents the values below 10% of the maximum (74.5 mVrms). In normalized data: dark red color on the color bar represents the maximum value (2.0 arbitrary units) and white color represents the values below 10% of the maximum (0.2 arbitrary units).

represents the maximum value (2.1 arbitrary units), and white color represents the values below 10% of the maximum (0.21 arbitrary units).

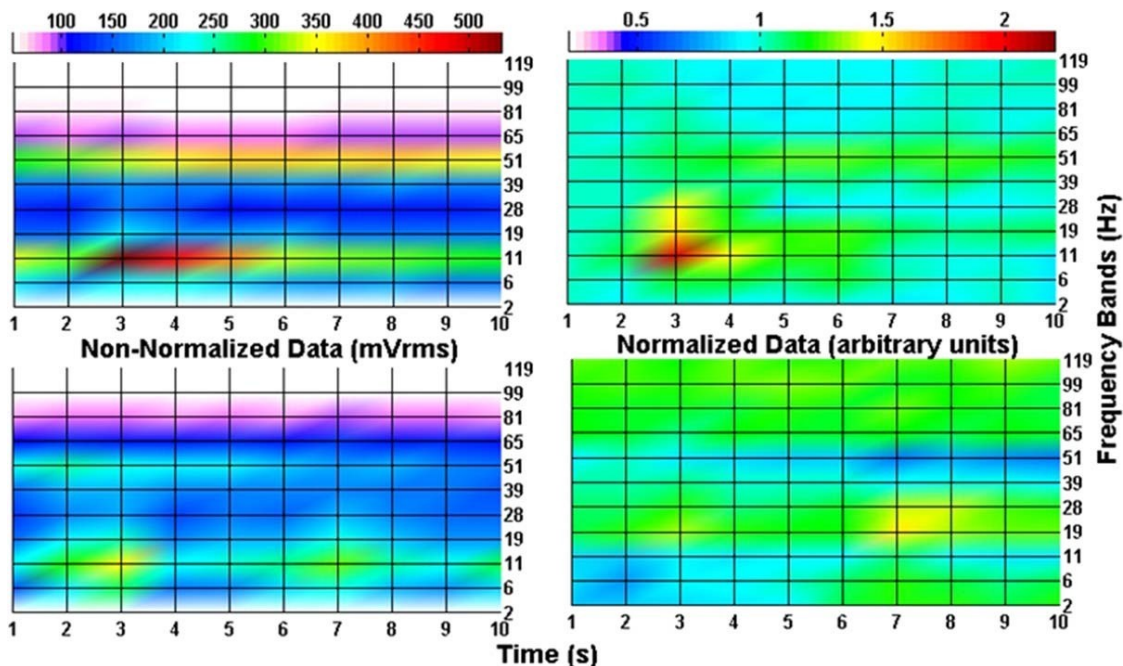


Fig. 7. The 2D MMG time-frequency responses (averaged) of the vastus medialis muscle during FES-induced isometric contraction: non-normalized (left images) and normalized (right images) data. In the top images: the initial segment followed by additional 6 s (non-fatigued); in the bottom images: the final segment with previous 6 s (fatigued). In non-normalized data: dark red color on the color bar represents the maximum value (531 mVrms), and white color represents the values below 10% of the maximum (53.1 mVrms). In normalized data: dark red color on the color bar represents the maximum value (2.2 arbitrary units), and white color represents the values below 10% of the maximum (0.22 arbitrary units).

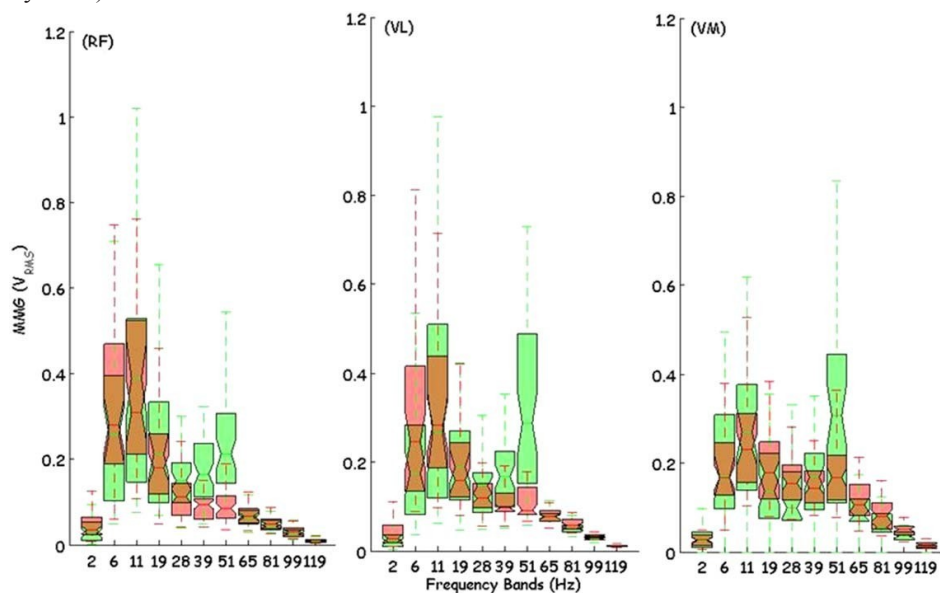


Fig. 8. Boxplot representation of CaW pseudo-frequencies for all subjects. RF: rectus femoris; VL: vastus lateralis; VM: vastus medialis. Green color: initial segment (4 s). Pink color: final segment (4 s). Brown color: superimposed data.

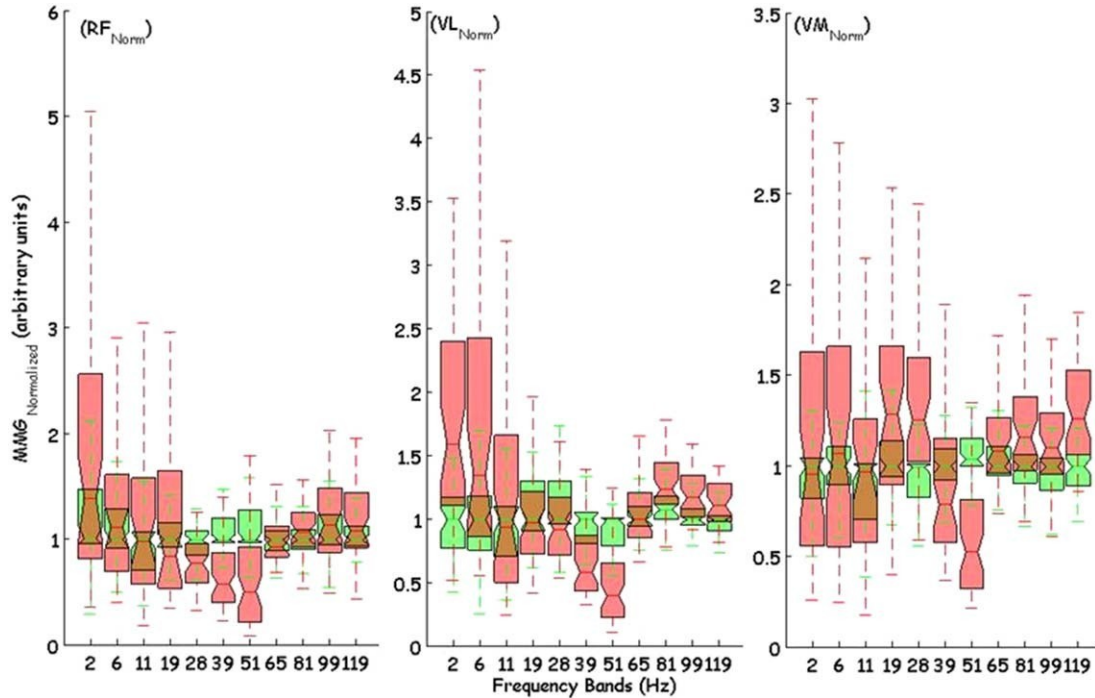


Fig. 9. Boxplot representation of CaW pseudo-frequencies for normalized data for all subjects. RF: rectus femoris; VL: vastus lateralis; VM: vastus medialis. Green color: initial segment (4 s). Pink color: final segment (4 s). Brown color: superimposed data.

In the final observation segment (fatigued muscle), there is an increase in energy concentration at lower frequencies (2 and 6 Hz) mainly during the last 4 s of the protocol recordings. These results are in accordance with Vaz et al. (50) who studied muscle fatigue with MMG in able-bodied volunteers and concluded that the increase of low-frequency energies is associated with the tremor that typically occurs toward the end of exhausting isometric contractions. Moreover, SCI people reach muscle fatigue much more rapidly than able-bodied people as found by Gerrits et al. (21), but with the same MMG response tendency when muscle fatigue develops.

The results indicated that after approximately 82.94 ± 6 43.22 s of FES application in SCI subjects, the MMG peak energy concentration shifted toward low frequencies, mainly below 11 Hz. This frequency shift coincided with the inability of FES to keep the knee joint angle at 58; therefore, the frequency shift toward lower frequencies was a clear indication of muscle fatigue. According to Bigland-Ritchie and Woods (51), muscle fatigue is any reduction in the force generating capacity of the total neuromuscular system regardless of the force required in any given situation. Moreover, the decrease in MMG frequency (32,52) can occur due to the motoneuron adaptation (53), that is, there is an increase in the depolarization threshold in response to constant stimulus (54). This biophysical event occurs through Na1 channels inactivation (55,56), which characterizes motoneuron adaptation during the prolonged application of electrical stimulation (13). Another possible reason is the motor unit coherence (57), that is, motor units contract in the phase leading to the shift of energy to lower frequency bands. Physiologically, it can occur when the vibration frequencies of contracting myofibers are the same or very close (i.e., below 11 Hz).

The increase in RMS values in frequency bands of 2 and 6 Hz are in contrast with our initial hypothesis that signal RMS amplitude should decrease with developing fatigue because there is no possibility for recruitment of new motor units in the paralyzed muscle stimulated with constant pulse intensities. However, total power in all frequency bands decreased from RF_{INI} 1.6 6 1.3 V to RF_{FIN} 1.3 6 0.9 V, VL_{INI} 1.6 6 1.2 V to VL_{FIN} 1.3 6 0.8 V, VM_{INI} 1.6 6 1.1 V to VM_{FIN} 1.4 6 0.6 V (median 6 interquartile range) which is in favor of the theory of motor unit coherence, where some MUs cease firing and others start firing in phase.

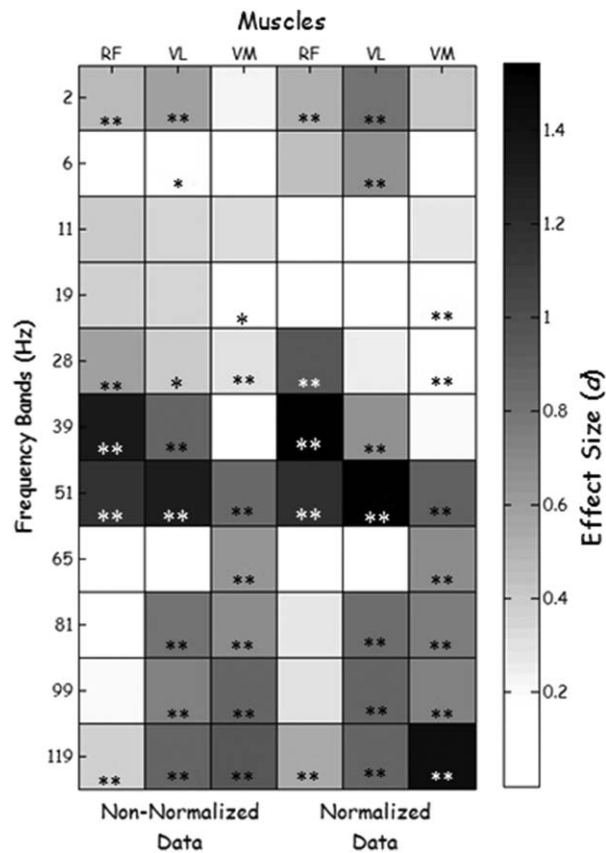


Fig. 10. Wilcoxon signed-rank test and effect size for the difference between CaW frequency bands' power in the initial (4 s) and final (4 s) segment. RF: rectus femoris; VL: vastus lateralis; VM: vastus medialis; *: $P < 0.05$; **: $P < 0.01$.

CONCLUSION

The Cauchy wavelet transform of MMG recordings from non-fatigued quadriceps muscle in SCI volunteers during sustained quasi-isometric contraction induced by FES (1 kHz frequency pulses, 3 ms-active cycle, and burst frequency of 50 Hz) revealed the highest energy concentration in the frequency band of 11 Hz. A possible reason may be the change in axonal physiology and morphology after a spinal cord injury, such as diameter axon reduction and the reduction in the

firing rate. Muscle fatigue was monitored by an electrogoniometer, and the fatigue instant was defined as the moment when the knee angle increased from the initial 58 to more than 208 of flexion. MMG wavelet analysis revealed an abrupt shift of energy concentration toward lower frequency bands (i.e., 2 and 6 Hz) several seconds before the contractile failure of the muscle due to fatigue. These findings show that MMG can be used as a real-time indicator of muscle fatigue during FES because: (i) MMG is immune to EMI induced by FES, (ii) a sudden change of the dominant frequency band several seconds before the contractile muscle failure leaves enough time to alarm the user and avoid disastrous consequences. Currently, there is no reliable and robust wearable sensor and method for muscle fatigue detection in paralyzed muscles during activity induced by neural prostheses. Our findings suggest that MMG can be used for fatigue detection in FES closed-loop systems for standing and walking (28–30,58) as a safety alarm for prevention of falls, or in other closed-loop FES systems as a form of biofeedback. More investigation is required to confirm the similar findings in case of non-isometric contractions and test algorithm efficacy in the case of significant motion artifacts which are also located in lower frequency bands. Further studies are required applying different FES parameters and electrodes placements. The precise allocation of dominant frequencies in 11 Hz and 2–6 Hz frequency bands in our results was consistent in the entire SCI group included in the experimental essay. In a recent study (Papcke et al., in submission process) we proved that the MMG dominant frequency is not affected by FES frequency (20, 25, 30, 35, 40, 45, 50, 75, and 100 Hz) when other stimulation parameters are defined as described in the methods section. In case of conventional biphasic stimulation (non-Russian Stimulation mode), the dominant frequency band may not be 11 Hz; however, there is a strong evidence from other studies, as well from our conducted additionally, unpublished study, for energy shift from higher to lower frequencies. Proper positioning of the sensors is important for observing of particular muscle behavior. As adhesive tape is not feasible for fixing sensors in daily practice, the sensor can be incorporated in elastic strap or a piece of tight clothing without impeding the measurements. Moreover, a grid of accelerometers in a garment positioned over the quadriceps may be a feasible solution that can release the user from restrictions in sensor positioning. Finally, MMG might find a purpose in studies for automated assessment of the recruitment parameters, such as stimulation thresholds, or useful ranges for stimulation frequency. It could be used for online modification of stimulation parameters to maintain fusion contraction with minimal applied stimulation frequency, for example, only when the shift toward lower frequencies is detected from MMG the stimulation frequency and/or amplitude should be increased.

Acknowledgments: We would like to thank Ana Carolina Moura Xavier Rehabilitation Center for allowing and providing the clinical setting to conduct this research and CNPq for scholarships and financial resources (Process n. 484325/2011-6). This work was partly supported by the Grant III 44008 from the Ministry of Education, Science and Technological Development of Serbia. Our acknowledgments to Vance Bergeron for English review.

Author Contributions: Eddy Krueger conceived the study, performed the protocols, signal acquisition, processing, and statistics. Percy Nohama conceived the study and supervised the protocols' application and with Lana Popović-Maneski participated in the design of the *in vivo*

study, and data analysis, and helped to draft the manuscript.

Conflict of Interest: The authors declare that they have no conflict of interests.

REFERENCES

1. Burt AA. The epidemiology, natural history and prognosis of spinal cord injury. *Curr Orthop* 2004;18:26–32.
2. Maynard FM, Bracken MB, Creasey G, et al. International standards for neurological and functional classification of spinal cord injury. *Spinal Cord* 1997;35:266–74.
3. Bedbrook GM. *The Care and Management of Spinal Cord Injuries*. New York: Springer, 1981.
4. Kern H, Carraro U, Adami N, et al. Home-based functional electrical stimulation rescues permanently denervated muscles in paraplegic patients with complete lower motor neuron lesion. *Neurorehabil Neural Repair* 2010;24:709–21.
5. Marsolais EB, Kobetic R. Functional electrical stimulation for walking in paraplegia. *J Bone Joint Surg* 1987;69:728–33.
6. Langzam E, Nemirovsky Y, Isakov E, Mizrahi J. Muscle enhancement using closed-loop electrical stimulation: volitional versus induced torque. *J Electromyogr Kinesiol* 2007; 17:275–84.
7. Kesar TM, Perumal R, Jancosko A, et al. Novel patterns of functional electrical stimulation have an immediate effect on dorsiflexor muscle function during gait for people post-stroke. *Phys Ther* 2010;90:55–66.
8. Gollee H, Hunt KJ, Wood DE. New results in feedback control of unsupported standing in paraplegia. *IEEE Trans Neural Syst Rehabil Eng* 2004;12:73–80.
9. Baldi JC, Jackson R, Moraille R, Mysiw WJ. Muscle atrophy is prevented in patients with acute spinal cord injury using functional electrical stimulation. *Spinal Cord* 1998;36: 679.
10. Guest RS, Klose KJ, Needham-Shropshire BM, Jacobs PL. Evaluation of a training program for persons with SCI paraplegia using the ParastepVR 1 ambulation system: part 4. Effect on physical self-concept and depression. *Arch Phys Med Rehabil* 1997;78:804–7.
11. Nash MS, Jacobs PL, Montalvo BM, Klose KJ, Guest RS, Needham-Shropshire BM. Evaluation of a training program for persons with SCI paraplegia using the ParastepVR 1 ambulation system: part 5. Lower extremity blood flow and hyperemic responses to occlusion are augmented by ambulation training. *Arch Phys Med Rehabil* 1997;78:808–14.
12. Enoka RM, Duchateau J. Muscle fatigue: what, why and how it influences muscle function. *J Physiol* 2008;586:11–23.
13. Yu NY, Chang SH. The characterization of contractile and myoelectric activities in paralyzed tibialis anterior post electrically elicited muscle fatigue. *Artif Organs* 2010;34:E117–21.
14. Bigland-Ritchie B, Jones D, Woods J. Excitation frequency and muscle fatigue: electrical responses during human voluntary and stimulated contractions. *Exp Neurol* 1979;64: 414–27.
15. Vøllestad NK. Measurement of human muscle fatigue. *J Neurosci Methods* 1997;74:219–27.
16. Thrasher A, Graham GM, Popovic MR. Reducing muscle fatigue due to functional electrical stimulation using random modulation of stimulation parameters. *Artif Organs* 2005;29: 453–8.
17. Karu ZZ, Durfee WK, Barzilai AM. Reducing muscle fatigue in FES applications by stimulating with N-let pulse trains. *IEEE Trans Biomed Eng* 1995;42:809–17.
18. Graupe D, Suliga P, Prudian C, Kohn K. Stochastically-modulated stimulation to slow down muscle fatigue at stimulated sites in paraplegics using functional electrical stimulation for leg

extension. *Neurol Res* 2000;22:703–4.

19. Popović LZ, Malešević NM. Muscle fatigue of quadriceps in paraplegics: comparison between single vs. multi-pad electrode surface stimulation. *Conf Proc IEEE Eng Med Biol Soc*, 2009;2009:6785–8.
20. Maneski L, Malešević NM, Savić AM, Keller T, Popović DB. Surface-distributed low-frequency asynchronous stimulation delays fatigue of stimulated muscles. *Muscle Nerve* 2013;48:930–7.
21. Gerrits H, De Haan A, Hopman M, Van der Woude L, Jones D, Sargeant A. Contractile properties of the quadriceps muscle in individuals with spinal cord injury. *Muscle Nerve* 1999;22:1249–56.
22. Marion MS, Wexler AS, Hull ML. Predicting fatigue during electrically stimulated non-isometric contractions. *Muscle Nerve* 2010;41:857–67.
23. Chesler NC, Durfee WK. Surface EMG as a fatigue indicator during FES-induced isometric muscle contractions. *J Electromyogr Kinesiol* 1997;7:27–37.
24. Mizrahi J, Levy M, Ring H, Isakov E, Liberson A. EMG as an indicator of fatigue in isometrically FES-activated paralyzed muscles. *IEEE Trans Rehabil Eng* 1994;2:57–65.
25. Malešević NM, Popović LZ, Schwirtlich L, Popović DB. Distributed low-frequency functional electrical stimulation delays muscle fatigue compared to conventional stimulation. *Muscle Nerve* 2010;42:556–62.
26. Merletti R, Knaflitz M, De Luca CJ. Electrically evoked myoelectric signals. *Crit Rev Biomed Eng* 1992;19:293–340.
27. Nguyen R, Masani K, Micera S, Morari M, Popovic MR. Spatially distributed sequential stimulation reduces fatigue in paralyzed triceps surae muscles: a case study. *Artif Organs* 2011;35:1174–80.
28. Kralj AR, Bajd T. *Functional Electrical Stimulation: Standing and Walking after Spinal Cord Injury*. Boca Raton, FL: CRC Press, 1989.
29. Kobetic R, Marsolais EB. Synthesis of paraplegic gait with multichannel functional neuromuscular stimulation. *IEEE Trans Rehabil Eng* 1994;2:66–79.
30. Popović D, Radulović M, Schwirtlich L, Jauković N. Automatic vs hand-controlled walking of paraplegics. *Med Eng Phys* 2003;25:63–73.
31. Seki K, Ogura T, Sato M, Ichie M. Changes of the evoked mechanomyogram during electrical stimulation. *Annual Conference of the International Functional Electrical Stimulation Society*, Brisbane, 2003.
32. Tarata MT. Mechanomyography versus electromyography, in monitoring the muscular fatigue. *Biomed Eng Online* 2003;2:3.
33. Islam MA, Sundaraj K, Ahmad RB, Ahamed NU. Mechanomyogram for muscle function assessment: a review. *PLoS One* 2013;8:e58902.
34. Shin I, Ahn S, Choi E, et al. Fatigue analysis of the quadriceps femoris muscle based on mechanomyography. *Int J Precis Eng Manuf* 2016;17:473–8.
35. Cè E, Rampichini S, Esposito F. Novel insights into skeletal muscle function by mechanomyography: from the laboratory to the field. *Sport Sci Health* 2015;11:1–28.
36. Cè E, Rampichini S, Monti E, Venturelli M, Limonta E, Esposito F. Changes in the electromechanical delay components during a fatiguing stimulation in human skeletal muscle: an EMG, MMG and force combined approach. *Eur J Appl Physiol* 2016;116:911–8.
37. Decker M, Griffin L, Abraham L, Brandt L. Alternating stimulation of synergistic muscles during functional electrical stimulation cycling improves endurance in persons with spinal cord injury. *J Electromyogr Kinesiol* 2010;20: 1163–9.
38. Popovic D, Sinkjaer T. *Control of Movement for the Physically Disabled: Control for*

Rehabilitation Technology. New York: Springer Science & Business Media, 2012.

39. von Tscharner V. Intensity analysis in time-frequency space of surface myoelectric signals by wavelets of specified resolution. *J Electromyogr Kinesiol* 2000;10:433–45.
40. Beck TW, von Tscharner V, Housh TJ, et al. Time/frequency events of surface mechanomyographic signals resolved by nonlinearly scaled wavelets. *Biomed Signal Process Control* 2008;3:255–66.
41. Krueger E, Scheeren E, Lazzaretti AE, Nogueira-Neto GN, Button VLSN, Nohama P, Cauchy wavelet-based mechanomyographic analysis for muscle contraction evoked by FES in a spinal cord injured person. In: IASTED, editor. *10th IASTED International Conference on Biomedical Engineering*, 2013 February 13–15, Innsbruck, Austria; 2013:237–42.
42. Ward AR, Robertson VJ, Ioannou H. The effect of duty cycle and frequency on muscle torque production using kilohertz frequency range alternating current. *Med Eng Phys* 2004;26:569–79.
43. Moreno-Aranda J, Seireg A. Investigation of over-the-skin electrical stimulation parameters for different normal muscles and subjects. *J Biomech* 1981;14:587–93.
44. Schiefer MA, Triolo RJ, Tyler DJ. A model of selective activation of the femoral nerve with a flat interface nerve electrode for a lower extremity neuroprosthesis. *IEEE Trans Neural Rehabil Syst Eng* 2008;16:195–204.
45. Burke D, Howells J, Trevillion L, McNulty PA, Jankelowitz SK, Kiernan MC. Threshold behaviour of human axons explored using subthreshold perturbations to membrane potential. *J Physiol* 2009;587:491–504.
46. Reilly JP. *Electrical Stimulation and Electropathology*. Cambridge: Cambridge University Press, 1992.
47. Cohen J. *Statistical Power Analysis for the Behavioral Sciences*. New York: Academic Press, 2013.
48. Bellemare F, Woods JJ, Johansson R, Bigland-Ritchie B. Motor-unit discharge rates in maximal voluntary contractions of three human muscles. *J Neurophysiol* 1983;50: 1380–92.
49. Nashmi R, Fehlings M. Changes in axonal physiology and morphology after chronic compressive injury of the rat thoracic spinal cord. *Neuroscience* 2001;104:235.
50. Vaz M, Zhang Y-T, Herzog W, Guimaraes A, MacIntosh B. The behavior of rectus femoris and vastus lateralis during fatigue and recovery: an electromyographic and vibromyographic study. *Electromyogr Clin Neurophysiol* 1996;36: 221–30.
51. Bigland-Ritchie B, Woods J. Changes in muscle contractile properties and neural control during human muscular fatigue. *Muscle Nerve* 1984;7:691.
52. Krueger-Beck E, Scheeren E, Nogueira-Neto GN, Button VLSN, Nohama P, Mechanomyographic Response during FES in Healthy and Paraplegic Subjects. *32nd Annual International Conference of the IEEE Engineering in Medicine and Biology Society (EMBC)*, 2010 August 31–September 4; Buenos Aires, Argentina: EMB, 2010:626–9.
53. Gandevia SC, Enoka RM, McComas AJ, Stuart DG, Thomas CK. *Fatigue: Neural and Muscular Mechanisms*. New York: Springer US, 1995.
54. Peron S, Gabbiani F. Spike frequency adaptation mediates looming stimulus selectivity in a collision-detecting neuron. *Nat Neurosci* 2009;12:318–26.
55. Hille B. *Ionic Channels of Excitable Membranes*, 2nd Edition. Sunderland: Sinauer, 1991.
56. Hodgkin AL, Huxley AF. The dual effect of membrane potential on sodium conductance in the giant axon of *Loligo*. *J Physiol* 1952;116:497–506.
57. Yao W, Fuglevand RJ, Enoka RM. Motor-unit synchronization increases EMG amplitude and decreases force steadiness of simulated contractions. *J Neurophysiol* 2000;83: 441–52.
58. Popovic D, Tomovic R, Schwirtlich L. Hybrid assistive system-the motor neuroprosthesis. *IEEE Trans Biomed Eng* 1989;36:729–37.